Data-driven multi-index overlay gold prospectivity mapping using geophysical and remote sensing datasets

Forson, E.D*[a]., Wemegah, D.D[b]., Hagan, G. B[a]., Appiah, D[c]., Addo-Wuver, F[c]., Adjovu, I[d]., Otchere, F. O[b]., Mateso, S[e]., Aboagye, M[b]., Amponsah, T[b]

[a]Department of Physics, University of Ghana [b]College of Science, KNUST, Kumasi-Ghana
[c]Department of Physics, UEW, Winneba-Ghana [d]Geodita Resources Limited, Accra-Ghana
[e]Department of Environmental Engineering and Management, The University of Dodoma, Tanzania

*Corresponding author's email:edforson@ug.edu.gh

Abstract

In this study, prospective zones of gold mineralization occurrences over the southern Kibi-Winneba belt have been delineated. This was preceded by using the prediction-area (P-A) plot by the generation of intersection points of prediction rate indicators that were essential in obtaining the normalized densities, which were subsequently used in generating the objective weight for each evidential layer in a data-driven way. The P-A and the normalized density techniques used were vital in recognizing the indicator and non-indicator criteria. The results obtained acknowledged the potassium concentration layer as a non-indicator of gold mineralization within the study area and subsequently recognized the hydroxyl concentration layer as the most plausible indicator criteria among the five indicator criteria (lineament density, iron concentration, hydroxyl concentration, gravity anomaly and magnetic anomaly) used. The indicator criteria were then integrated to generate a mineral prospectivity map (MPM) over the study area.

Introduction

The southern Kibi-Winneba belt, though a prominent gold (Au) belt in Ghana, still remains an under-explored virgin area and hence there is the need for a mineral potential map to guide various exploration programs essentially geared toward unraveling its mineralization prospects (Klemd et. al., 2002). In view of this, the normalized density would be used to calculate the objective weights based on known Au occurrence with respect to 6 evidential layers, to generate a mineral prospectivity map (MPM) in a data-driven manner.

Geological Setting

Geologically, the area under investigation covers the southern Kibi-Winneba belt, which falls within the Central Region of Ghana. It generally encompasses Birimian metavolcanics, metasediments and granitoids. The mineralization style of the study is generally structurally controlled with predominance of quartz vein deposit (Klemd et. al., 2002).

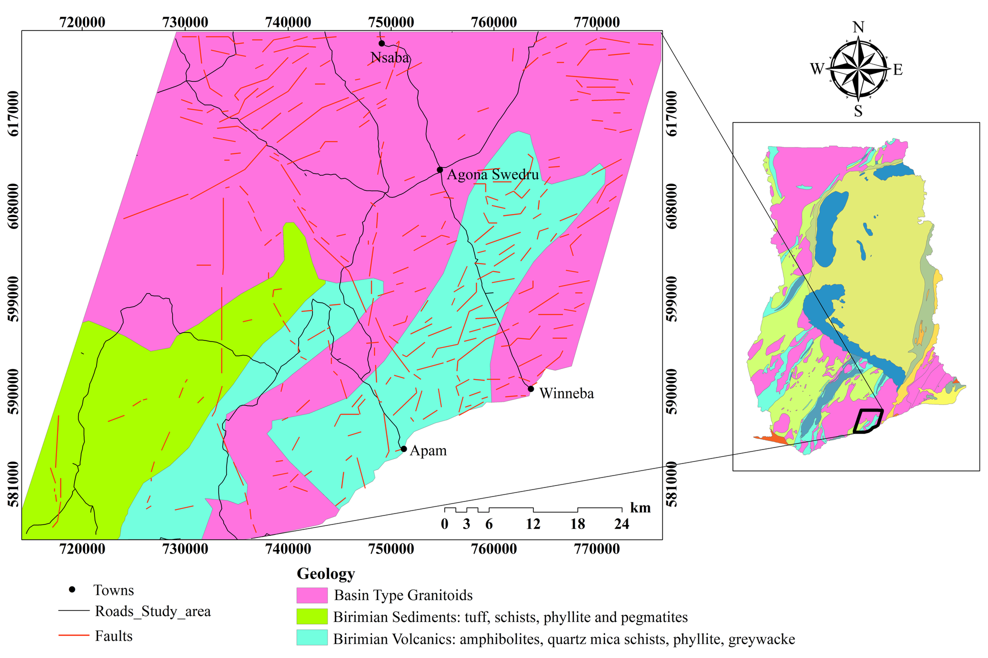

Figure 1: Geological map of the southern Kibi-Winneba belt (modified from Klemd et. al., (2002))

Method

Datasets

In this study, six geospatial evidential layers (EVLs) encompassing magnetic anomaly (Mag), gravity anomaly (Grav), potassium concentration (K), hydroxyl concentration (OH), iron concentration (Fe) and lineament density (LD) were used. The magnetic and lineament density layers were generated from aeromagnetic data, whereas the potassium concentration layer was generated from aero-radiometric data that were obtained from the Ghana Geological Survey Authority. The gravity anomaly layer was obtained from Bouguer gravity map from the GFZ German Research Centre for Geosciences (www.gfz-potsdam.de). The iron and hydroxyl concentration layers were obtained from the Landsat 8 OLI remote sensing data from the United States Geological Survey Earth Resources Observation and Science Center (www.usgs.gov/centers/eros). 36 known locations of gold occurrences were used as ground truth.

Generation of continuous evidential layers

The spatial values of the 6 EVLs were transformed based on the logistic function owing to its efficacy to properly transform boundless values into a range of 0-1 (equation 2).

$$f_{ij} = \frac{1}{1+e^{-s(a_{ij}-i)}}, i = 1, 2, \cdots, m, \; j = 1, 2, \cdots, n \tag{1}$$

$$A = \begin{bmatrix} a_{11} & a_{12} & \cdots & a_{1n} \\ a_{21} & a_{22} & \cdots & a_{2n} \\ \vdots & \vdots & \ddots & \vdots \\ a_{m1} & a_{m2} & \cdots & a_{mn} \end{bmatrix} = [a_{ij}]_{m\times n} \tag{2}$$

From equation 1, i, f_{ij} and s respectively denote the point of inflexion, transformed value of i alternative with respect to j criterion and the slope. Defining the values for i and s involve objectivity so as to confine the transformed values in the range 0 to 1 (Yousefi and Carranza, 2015).

Discretization of evidential layers based on concentration-area (C-A) fractal model

The concentration-area (C-A) fractal model (equation 3) proposed by Cheng et. al., (1994) was employed in a data-driven manner instead of the arbitrary manner to define the thresholds viable for discretizing various continuous evidential layers so as to generate corresponding layers or maps in a classified manner.

$$\begin{aligned} A(\rho \leq v) \propto \rho^{-\alpha_1} \\ A(\rho \geq v) \propto \rho^{-\alpha_2} \end{aligned} \tag{3}$$

$A(\rho)$ depicts the area of concentrated values higher than or equal to contour value ρ (value of each pixel of an evidential layer); α_1 and α_2 represents the minimum and maximum characteristic exponents respectively and the v is breakpoint or threshold.

Generation of prediction-area (P-A) plots from evidential layers

The prediction-area (P-A) plot is efficient in delineating the possible occurrence of a particular mineral deposit by correlating the number of mineral occurrences available in relation to the variously delineated classes of prospectivity within a particular region of interest. This was achieved by superimposing the 36 locations of Au occurrences over each of the discretized evidential layers as well as the finally produced MPM.

Weighting of evidential layers based on normalized density

The objective weights of the EVs were calculated using equations 4 and 5

$$N_d = \frac{P_r}{O_a} \tag{4}$$

N_d, P_r *and* O_a denote respectively the normalized density, prediction-rate and the occupied area derived from the point of intersection in P-A plots generated for various evidential layers.

$$W_E = ln\ N_d \tag{5}$$

W_E denotes the objective weight calculated for an evidential layer based on parameters obtained from the point of intersection in a P-A plot.

Integration of Evidential Layers

$$DM_{IO} = \frac{\sum_i^n TV_i W_{Ei}}{\sum_i^n W_{Ei}} \tag{6}$$

DM_{IO} represents the multi-index overlay score in the data-driven way; W_{Ei} and T_{Vi} represent respectively the weight of an evidential layer and pixel value of logistic function-transformed evidential layer i.

Results

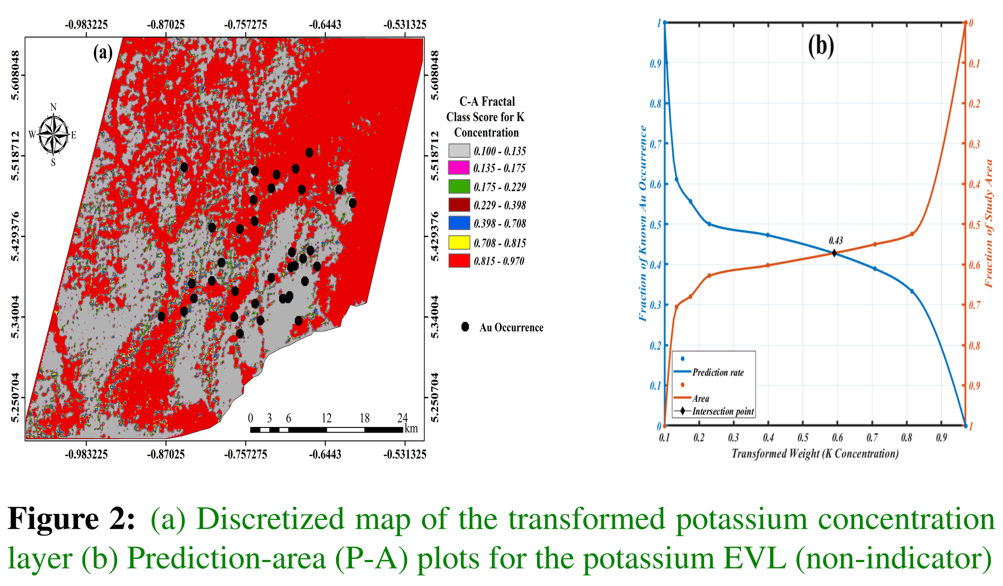

Figure 2: (a) Discretized map of the transformed potassium concentration layer (b) Prediction-area (P-A) plots for the potassium EVL (non-indicator)

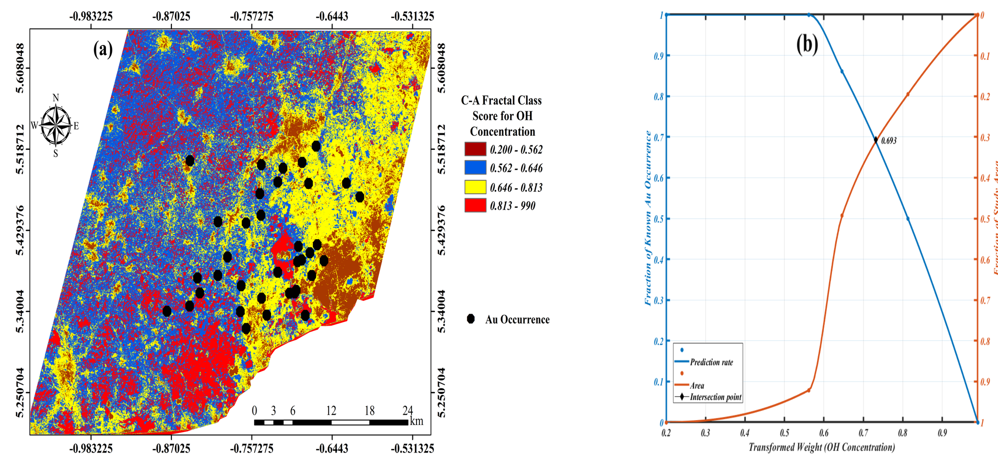

Figure 3: (a) Discretized map of the transformed hydroxyl EVL (b) Prediction-area (P-A) plots for the hydroxyl EVL (highest among the indicators)

Table 1: Generated weights of each evidential layer based on the normalized density technique

EVL	P_r	O_a	N_d	W_E
LD	0.586	0.414	1.42	0.35
K	0.430	0.570	0.75	-0.29
OH	0.693	0.307	2.26	0.61
Fe	0.680	0.320	2.13	0.76
Grav	0.630	0.370	1.70	0.53
Mag	0.520	0.480	1.08	0.08

The indicator EVLs ($W_E > 0$) were integrated using equation 6 to produce the mineral prospectivity map. The mineral prospectivity map generated was discretized into 5 classes to produce the C-A fractal discretized index overlay prospectivity map (Figure 4a).This produced prospectivity scores: 0.202 - 0.479, 0.479 - 0.646; 0.646 - 0.794; 0.794 - 0.891 and 0.891 - 0.985 with an area coverages of $334.613\,\text{km}^2$, $687.512\,\text{km}^2$, $734.48\,\text{km}^2$, $313.048\,\text{km}^2$ and $105.151\,\text{km}^2$ respectively. From Figure 4b, the prediction rate obtained was 0.764, which is higher than the prediction rates for the individual evidential layers (Table 1). This implies that, the multi-index overlay technique increases the prediction rate [i.e., 0.764 > (0.693, 0.68, 0.630, 0.586, 0.52)] for the final prospectivity map based on the integration of the indicator criteria and hence makes the use of continuously transformed values of evidential layers essential in the mineral prospectivity mapping.

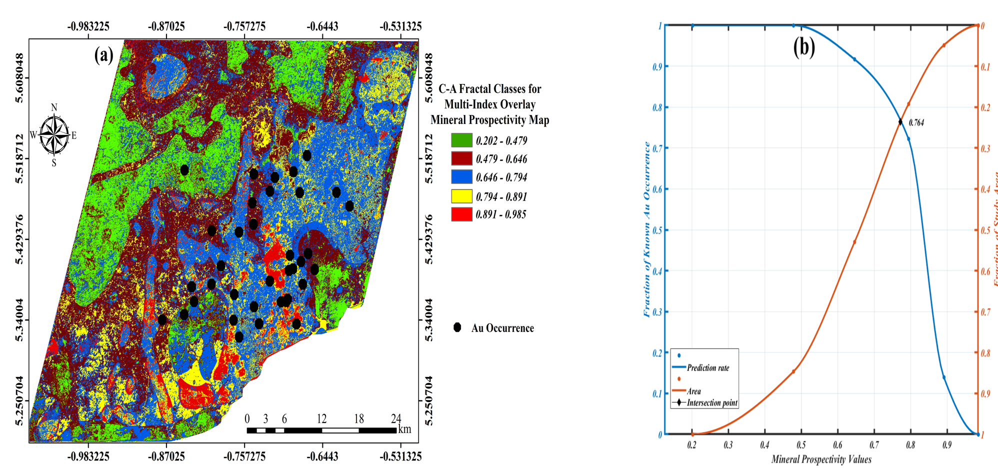

Figure 4: (a) C-A fractal model based discretized multi-index overlay prospectivity map (b) Prediction-area (P-A) plots for the MPM generated

Conclusions

Objective weights for 6 evidential layers comprising magnetic anomaly, gravity anomaly, potassium concentration, hydroxyl concentration, iron concentration and lineament density were generated using the logistic function, concentration-area fractal model, prediction-area plots as well as the normalized density technique. The potassium concentration was delineated as a non-indicator, with its$W_E = -0.29$ (less than 0) and hence was not included in the generation of the mineral prospectivity map (MPM). The final MPM produced indicated that, 23.6% of the study area is prospective, within with 76.4% of the known Au occurrences are observed.

References

- Klemd, R., Hnken, U., & Olesch, M. (2002). Metamorphism of the country rocks hosting gold?sulfide-bearing quartz veins in the Paleoproterozoic southern Kibi-Winneba belt (SE-Ghana). Journal of African Earth Sciences, 35(2), 199-211
- Cheng, Q., Agterberg, F. P., & Ballantyne, S. B. (1994). The separation of geochemical anomalies from background by fractal methods. Journal of Geochemical exploration, 51(2), 109-130.
- Yousefi, M., & Carranza, E. J. M. (2015). Prediction?area (P?A) plot and C?A fractal analysis to classify and evaluate evidential maps for mineral prospectivity modeling. Computers & Geosciences, 79, 69-81.